Nanoscale

Accepted Manuscript

This article can be cited before page numbers have been issued, to do this please use: S. Portillo, J. Cervera, J. A. Manzanares, J. Bisquert, S. Mafe and P. Ramirez, *Nanoscale*, 2026, DOI: 10.1039/D6NR00934D.

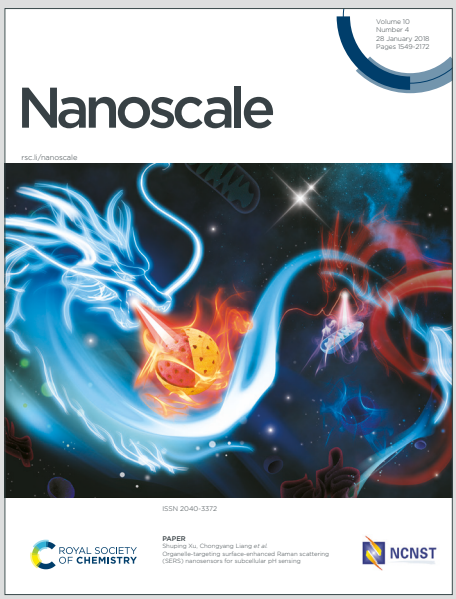

ROYAL SOCIETY OF CHEMISTRY

rsc.li/nanoscale

View Article Online
DOI: 10.1039/D6NR00934D

Iontronics of nanofluidic conical pores: learning phenomena using voltage pulses

Sergio Portillo,[1,a)] Javier Cervera[1], José A. Manzanares[1], Juan Bisquert[2], Salvador Mafe,[1,3] Patricio Ramirez[4,b)]

[1]*Dept. de Física de la Terra i Termodinàmica, Universitat de València, E-46100 Burjassot, Spain*

[2]*Instituto de Tecnología Química (Universitat Politècnica de València-Agencia Estatal Consejo Superior de Investigaciones Científicas), 46022 València, Spain.*

[3]*Allen Discovery Center at Tufts University, Massachusetts, USA*

[4]*Dept. de Física Aplicada, Universitat Politècnica de València, E-46022 València, Spain*

a) Corresponding author: E-mail: sergio.portillo@uv.es
b) Corresponding author: E-mail: patraho@fis.upv.es

View Article Online
DOI: 10.1039/D6NR00934D

ABSTRACT

Nanofluidic memristors exhibit conductance memory effects that can be used in neuromorphic computing, an emerging technology reminiscent of the brain synapses that change their connection strength in response to electrical signals. We describe different options allowing the modulation of the nanofluidic conductance by programming series of rectangular voltage pulses of different characteristics, amplitude, duration, and frequency. The resulting history-dependent conductance allows short-term memory states and learning procedures through potentiation (connection strengthening) and depression (connection weakening) effects. In addition, electrochemical networks of nanofluidic memristors provide operational procedures to implement both logical responses and reservoir computing algorithms using different series of voltage pulses as inputs. As a proof of concept, the supervised learning of a nanofluidic memristive array allows playing a tic-tac-toe game.

View Article Online
DOI: 10.1039/D6NR00934D

I. INTRODUCTION

Micro and nanofluidic ionics permit physical environments, electrical carriers, and spatio-temporal scales that mimic biological synapses in neuromorphic computing, thus constituting a scalable soft-matter hardware reminiscent of brain synapse plasticity. Nanoscale channels typically show fixed charges on the pore surface that attract counterions (mobile ions with charge sign opposite to that of the pore surface charges) and repel coions (mobile ions with the same charge sign as these surface charges) from the external salt solution, forming an electric double layer responsive to external electric fields. These experimental facts allow the use of different physico-chemical options to modulate the system electrical response.[1–5] In particular, the application of a potential difference (voltage) and the measurement of the resulting electric current constitutes a basic method in iontronics. When subjected to a series of voltage pulses, nanofluidic memristors exhibit memory effects that depend on the particular history of the external stimulation, which can be used in neuromorphic computing applications that mimic biological synapses.[6–23] The switching between different pore conductance states can be established within short experimental times, analogous to brain synapses changing their connection strength in response to fast electrical signals.

We describe here different procedures that allow for the conductance modulation of conical nanofluidic diodes[2,24,25] by programming different series of rectangular voltage pulses, which can constitute a useful guide to future neuromorphic computing applications. These applications are based on the fact that the spatio-temporal distribution of the mobile ions in the pore depends on the characteristics (amplitude, duration, and frequency) of the voltage pulses.[7,21,22] In particular, the

View Article Online
DOI: 10.1039/D6NR00934D

different voltage signs lead to distinct accumulation and depletion phenomena that modulate the pore conductance in terms of the nanoscale ionic concentration.[26] Because the conductance state at a given time depends on the previous voltage inputs, short-term memory and learning phenomena can be implemented through potentiation (connection strengthening) and depression (connection weakening) sequences, which are reminiscent of the plasticity of biological synapses.[6–8,12,19]

The manuscript describes both theoretically and experimentally the use of voltage pulses in neuromorphic computing for significantly different tasks that include logical functions and playing a tic-tac-toe game. A complete physico-chemical characterization, which includes current-voltage curves, impedance, and voltage pulses, shows how the conical nanopores conductance can be modulated by the salt type and concentration, temperature, pH, and multivalent cations. Experimental data concerning the pore long-term stability are also included. Nanofluidic memristors could be used in electrochemical circuits that provide useful options for sensing and actuating, implementing logical functions, the conversion between ionic and electronic signals, and the learning of different patterns from distinct series of voltage pulses. In these cases, the pore ionic solution acts as a multi-purpose programmable synaptic unit[9–14,17,27–38] that is reminiscent of a biological memory in cell systems.[39–44]

II. NANOPORE CHARACTERIZATION

We briefly summarize the nanopores characteristics that have been described previously.[14,20] The conical pores consist of functionalized tracks in membranes of an exposed area of 1 cm^2. The tracks were obtained by irradiation of a polyimide foil by single swift heavy ions.[2,24,45,46] The subsequent

View Article Online
DOI: 10.1039/D6NR00934D

functionalization is achieved by asymmetric track-etching techniques that result in negatively-charged pores whose tip and base radii are of the order of 10 nm and 100 nm, respectively.[2] The pore surface charges are carboxylic acid moieties ionized in neutral pH salt solutions. Voltage (V) pulses result in current (I)–time (t) traces measured with an electrochemical cell that is located within a double-shielded Faraday cage mounted on an anti-vibration table (Figure 1a). The experimental I–V, I–t, and Im(Z) – Re(Z) impedance (Z) curves obtained for two typical membrane samples are shown in Figures 1b–1d. As expected from the I–V curves, the impedances are higher for voltages $V < 0$ than for $V > 0$.[46] Also, at $V > 0$ chemical inductance effects characterized by – Im(Z) < 0 (Fig. 1d) are observed.[46]

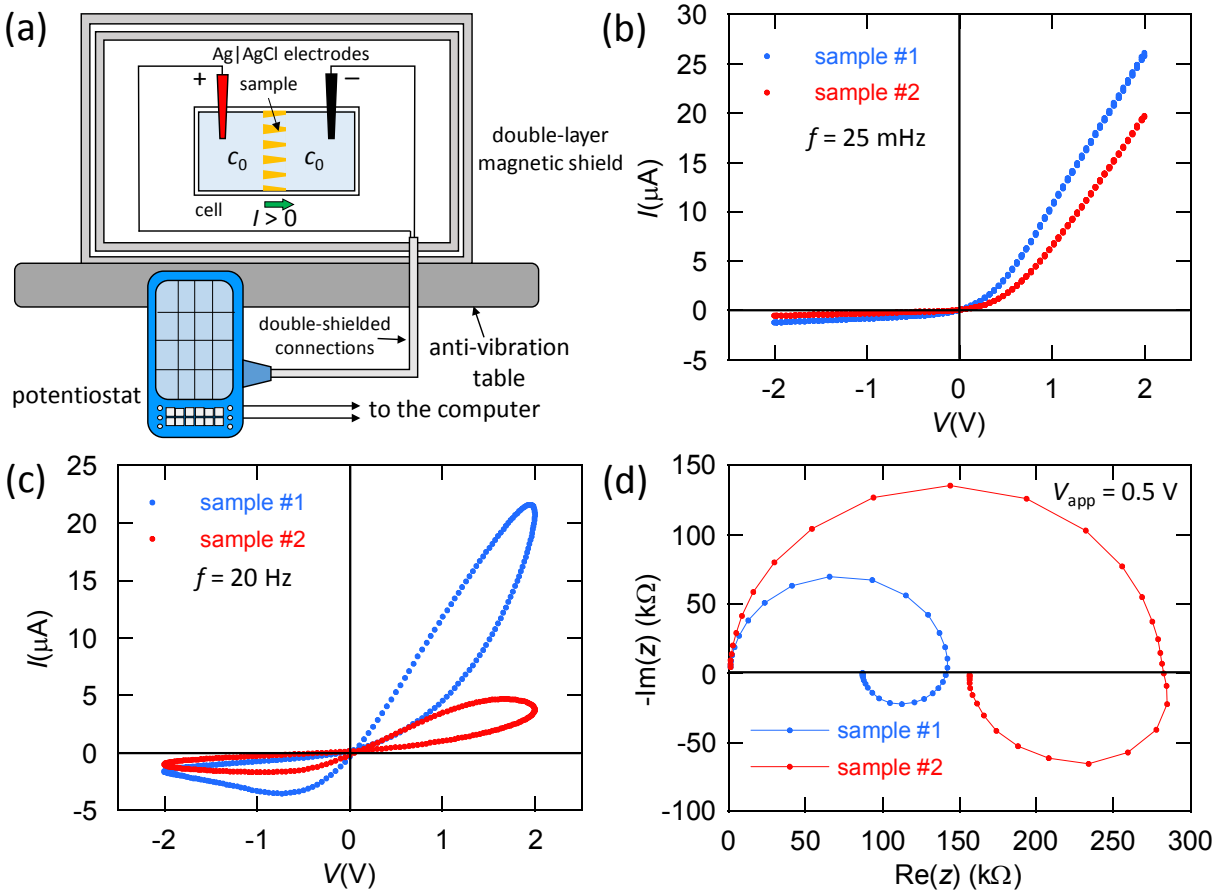

View Article Online
DOI: 10.1039/D6NR00934D

FIG. 1

(a) Experimental setup. (b) Experimental current (I) – voltage (V) steady-state curves for two different multipore membranes, samples #1 and #2 obtained with a slow triangular wave at the scan rate 200 mV/s corresponding to a cycle frequency of 25 mHz. Note the qualitatively similar results obtained for two different membrane samples. Also, the observed current rectification results from the conical charge distribution: ionic accumulation occurs at forward polarization ($V > 0$) while ionic depletion occurs at reverse polarization ($V < 0$). (c) The corresponding $I - V$ memristive curves obtained with a sinusoidal voltage of frequency 20 Hz. Note the significant memory effects observed for the two membranes. (d) The impedance Nyquist plots Im(Z) – Re(Z) for the two membranes. All measurements were conducted in aqueous solutions of concentration c_0 = 0.1 M KCl.

Figure 2 shows the I–V curves of membranes with 200 – 300 pores bathed in KCl solutions obtained with a sinusoidal voltage signal of frequency 20 Hz. In Figure 2a, different samples obtained in the same beam session show similar qualitative rectification characteristics in 100 mM KCl solutions. Note also that a moderate unit variability can improve the network performance in practical applications, as shown in Reference 14 and in the case of using different ionic solution concentrations here.

Figure 2b demonstrates that, by keeping the samples in a 100 mM KCl aqueous solution and avoiding extreme pH and temperatures, the membrane conductance remains stable for months. Hydration losses can also be recovered and, by further activation with EtOH, the samples remain operative for years. Figure 2c shows that the KCl solution concentration allows also a significant

View Article Online
DOI: 10.1039/D6NR00934D

modulation of the pore conductance. Figure 2d displays the increase of the membrane conductance with the temperature. Figure 2e suggests that at low pH the protonation of the fixed charge groups gives positive pore surface charges. On the contrary, at high pH the deprotonation of the fixed charge groups gives negative pore surface charges, thus reversing the pore rectification. Figure 2f shows the effects of the ionic adsorption on the pore surface: the divalent (Ca^{2+}) and trivalent (La^{3+}) cations can regulate the surface charge,[47] thus changing the pore rectification and memristive properties. These experimental facts extend the pore functionalities, as shown in Reference 22 and Figure 5 of the manuscript.

View Article Online
DOI: 10.1039/D6NR00934D

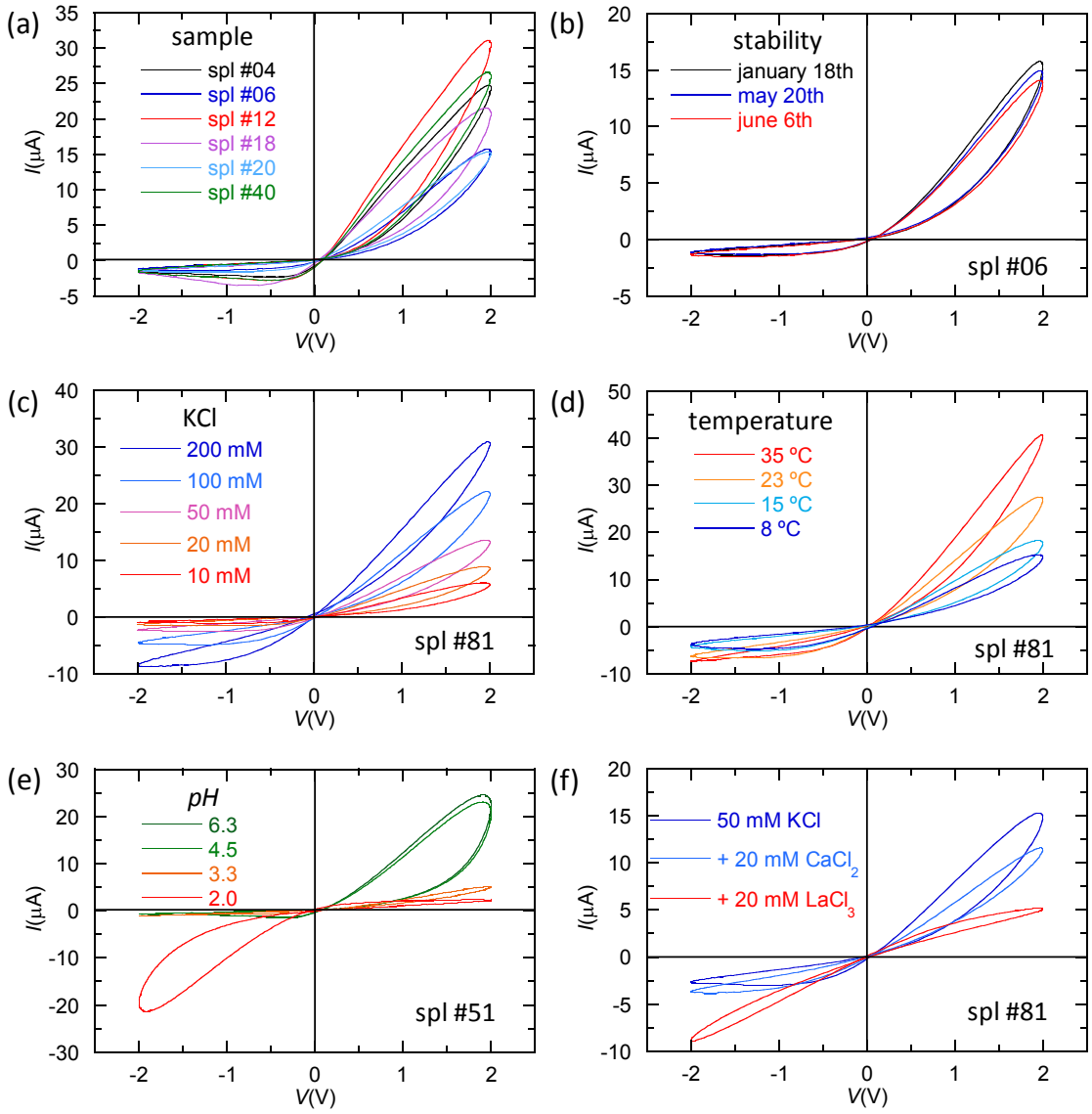

FIG. 2

(a) *I*–*V* curves of membranes with 200 – 300 pores bathed in 100 mM KCl solutions and measured with a sinusoidal voltage signal of frequency 20 Hz. The six different samples obtained in the same beam session show similar qualitative rectification characteristics. (b) By keeping the samples in the above aqueous solution and avoiding extreme pH and temperatures, the *I*–*V* curve remains stable for months. (c) The *I*–*V* curves measured at different KCl solution concentrations suggest a

View Article Online
DOI: 10.1039/D6NR00934D

significant modulation of the pore conductance. (d) The membrane conductance increases with temperature in a 100 mM KCl solution and a sinusoidal voltage signal of frequency 20 Hz. (e) The effect of pH on the $I–V$ curves: low pH values give positive surface charges while high pH values give negatively-charged pores, thus reversing the pore rectification. (f) The different salt type and distinct ionic adsorption phenomena can also regulate the pore surface charge, thus changing the membrane rectification and memristive properties.

Taken together, Figures 2a–2f suggest that environmental conditions such as the salt type and concentration, the temperature, and the pH are useful to modulate the pore conductance in practical applications. For instance, using the range $2 < \text{pH} < 8$ provides positive (acid pH) and negative (neutral pH) pore charges, thus changing the pore rectification characteristics[22] in relatively short times in the minute range. As to the continuous pore operation at constant ionic solution concentrations, frequency signals in the range of $10 - 50$ Hz have shown significant memristive effects previously.[14,22] In general, when the voltage switching is faster than the ionic relaxation at the conical pore tip, the accumulation and depletion phenomena give frequency-dependent $I - V$ curves with significant hysteresis. On the contrary, slow voltage sweeps eliminate memory effects because the ionic solution has time enough to equilibrate. Note however that extremely fast voltage switching can give linear responses because the ions cannot follow the rapid changes of the voltage signal and thus their motion becomes effectively frozen.

Concerning the energy balance, we can give only an order of magnitude estimation. The typical voltages and small nanopore currents involved suggest relatively low minimal

View Article Online
DOI: 10.1039/D6NR00934D

requirements, with an individual power dissipation of the order of 10 μA × 1 V = 10 μW per membrane. However, this estimation should be scaled up to the number of units in the network and may constitute a lower bound value because of the readout hardware requirements.

A direct comparison of the above liquid-state characteristics with much faster solid state devices based on electronic conduction would be of limited value because of their different nonlinear dynamics and electrical carriers, together with the distinct biochemical and biotechnological signal processing applications of nanofluidic iontronics. Also, we have not observed significant coupling between neighboring pores because of the relatively low surface pore density in the membranes together with the fact that we have not integrated the nanopores in a small microchip yet. In this context, we have carried out previously a thorough study of ionic circuitry with nanofluidic diodes[29] that suggests the additivity of current responses over different macroscopic pores and networks arrangements. Note also that extreme miniaturizations are not required in most chemical and biotechnological applications.

III. RESULTS AND DISCUSSION

We give first a full account of the membrane current and conductance responses to voltage pulses of different amplitude, time duration, and time separation characteristics to be used in different operational methods. The results provide a useful qualitative view of the effect of the pulse parameters on the pore short-time memory. Figure 3a shows the effect of the voltage pulse amplitude V_0 when the pulse time duration Δt_0 and the separation Δt between consecutive pulses are fixed. As expected, the membrane conductance increases with the pulse amplitude. Figure 3b

View Article Online
DOI: 10.1039/D6NR00934D

considers different time durations Δt_0 at fixed V_0 and Δt values. The conductance increases with Δt_0 because of the inductive nature of the current loops of Figure 1d.[20,22] Figure 3c introduces different separation times Δt at fixed V_0 and Δt_0 values. In this case, the conductance decreases with con Δt because of the decrease of the ionic accumulation with time following the pore solution relaxation. Figure 3d shows the effect of the KCl concentration c_0 at fixed V_0, Δt_0, and Δt. Clearly, the conductance increases with c_0 because of the concomitant increase in the number of electrical carriers present in the ionic solution. Figures 4a–4d show that the theoretical curves obtained with a previously described memristive model with the typical parameters for conical pores.[20,22] The comparison with the experimental data of Figures 3a–3d suggest that this model can be useful to guide future experiments and practical applications.

In general, the voltage-driven ion concentration polarization caused by transient pulse trains of typical 1 – 3 V amplitude and 1 – 100 ms duration provide relatively fast but volatile responses with limited time retention in the second to minute regime. Note however that the typical stable and non-volatile responses obtained in other systems tend to come at the price of slow switching. As to the typical times for diffusion along the long pore axis, they can be in the second regime while accumulation/depletion at the conical pore tip is much faster and occurs in the 1 – 10 ms regime.

View Article Online
DOI: 10.1039/D6NR00934D

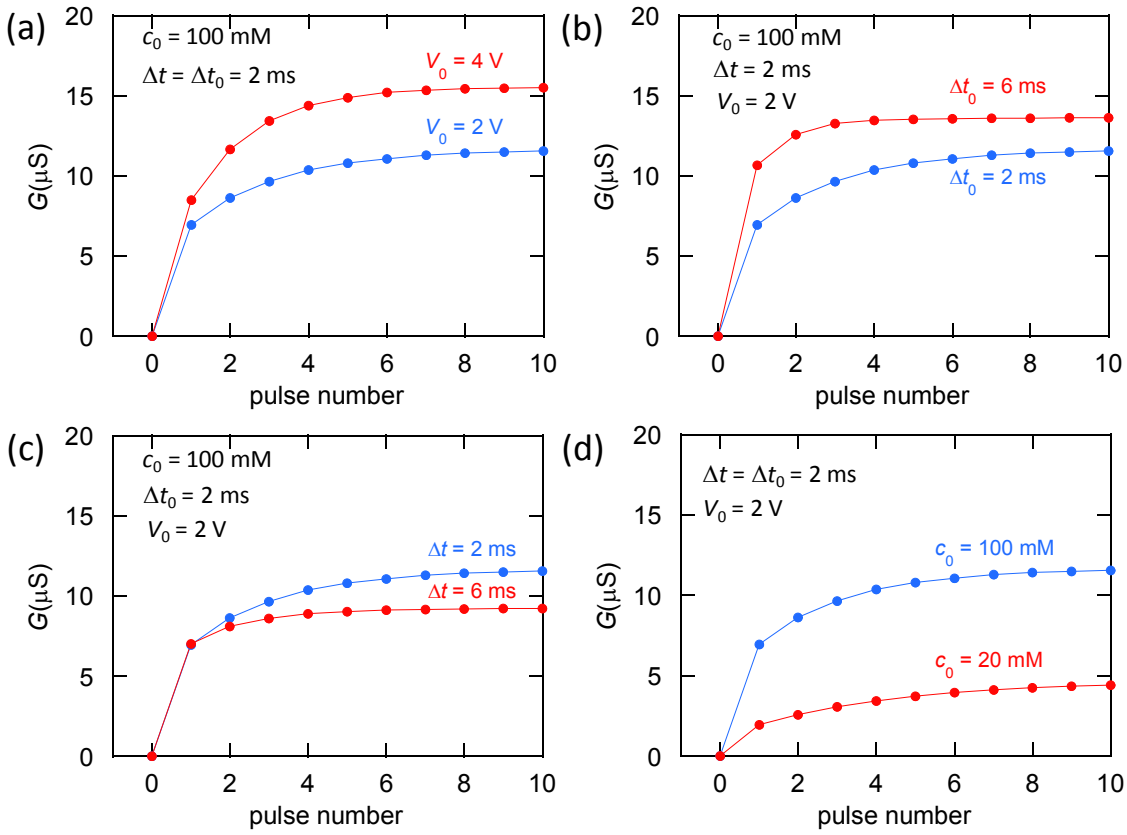

FIG. 3

(a) Conductance (G) – pulse number curve for membrane sample #1 immersed in a c_0 = 100 mM KCl aqueous solution parametrically in the amplitude V_0 of voltage pulses with time duration Δt_0 = 2 ms. The time separation between consecutive pulses is Δt = 2 ms. (b) G – pulse number curve parametrically in the time duration Δt_0 for V_0 = 2 V and Δt = 2 ms, with c_0 = 100 mM KCl. (c) G – pulse number curve parametrically in the separation time Δt between consecutive pulses for V_0 =2 V and Δt_0 = 2 ms, with c_0 = 100 mM KCl. (d) G – pulse number curve parametrically in the KCl concentration c_0 for V_0 = 2 V, Δt_0 = 2 ms, and Δt = 2 ms.

View Article Online
DOI: 10.1039/D6NR00934D

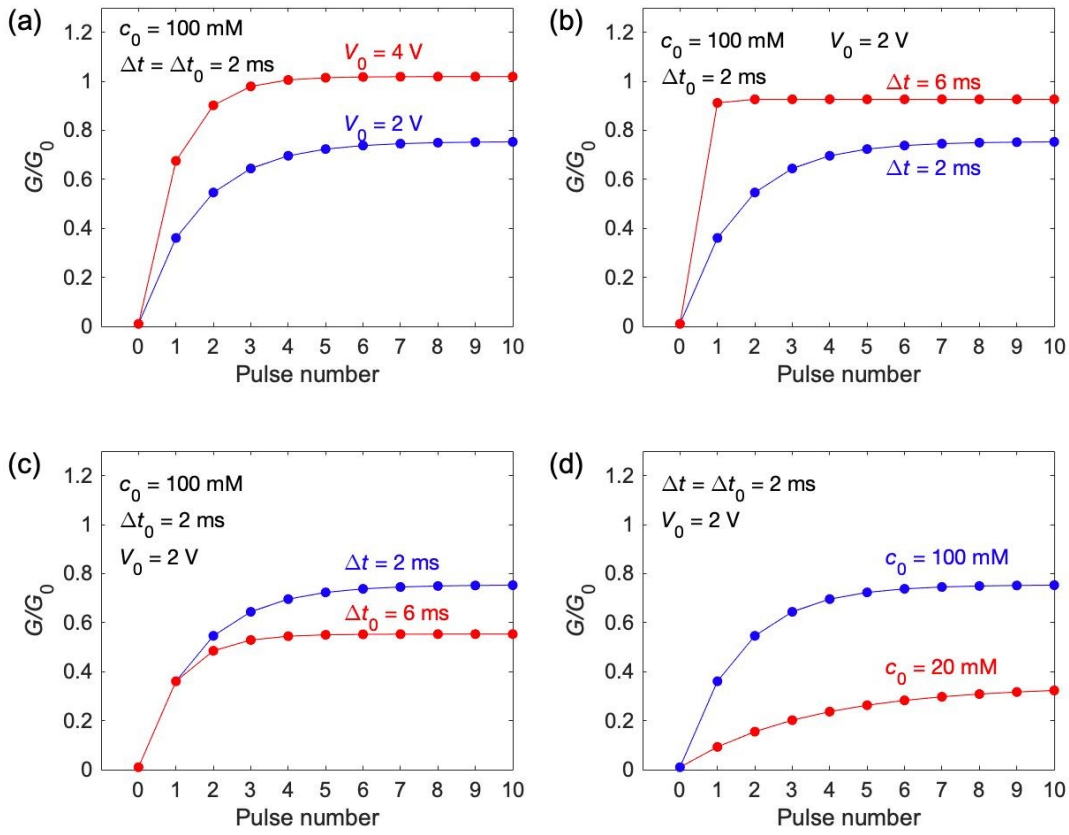

FIG. 4

(a) Theoretical dimensionless conductance (G/G_0) – pulse number curve for membrane sample #1 immersed in a c_0 = 100 mM KCl aqueous solution parametrically in the amplitude V_0 of voltage pulses with time duration Δt_0 = 2 ms (*inset*). Here, G_0 is a scaling theoretical conductance and the time separation between consecutive pulses is Δt = 2 ms. (b) (G/G_0) – pulse number curve parametrically in the time duration Δt_0 for V_0 = 2 V and Δt = 2 ms, with c_0 = 100 mM KCl. (c) (G/G_0) – pulse number curve parametrically in the separation time Δt between consecutive pulses for V_0 =2 V and Δt_0 = 2 ms, with c_0 = 100 mM KCl. (d) (G/G_0) – pulse number curve parametrically in the KCl concentration c_0 for V_0 =2 V, Δt_0 = 2 ms, and Δt = 2 ms.

View Article Online
DOI: 10.1039/D6NR00934D

A complete, full theoretical description of the effects of voltage signal amplitude, signal frequency, salt type, and ionic concentration showing a quantitative model match of the experimental data is given in Reference 22. Thus, we emphasize that a physical description of the experiments based on the dynamics of ions driven by electric pulses reproducing the non-linear and fading-memory properties of the nanopores can be obtained using a limited set of experimentally-accessible parameters, thus avoiding complex numerical fitting techniques.

The conductance potentiation can also be characterized from the Paired-Pulse Facilitation (PPF), measured as the relative conductance changes (in %) obtained by applying two consecutive pulses, PPF = $100\%(G_{\text{final}} - G_{\text{initial}})/ G_{\text{initial}}$. In this way, PPF describes the temporary increases (potentiation) or decreases (depression) observed in the current following a sequence of voltage pulses (Figures 5a–5d). This short-term memory effect where the second pulse elicits a different response than the first one is typical of neural systems and can also be replicated in nanofluidic pores.[48] However, different definitions have been employed and the PPF value obtained depends on the initial conductance state assumed. For instance, an initial reference state with high baseline conductance can exhibit a small PPF value compared to that of another case with lower initial conductance, despite similar potentiation capabilities.[48]

Figures 5a, 5b, and 5d show the PPF effect as a function of the pulse time separation Δt. The curves, which are parametric in the pulse voltage amplitude (Figure 5a), time duration Δt_0 (Figure 5b), and ionic solution concentration (Figure 5d), show the decrease of the potentiation with the pulse separation due to the significant decrease of the ionic accumulation between consecutive pulses. These results can be compared with those of Figure 3 for the membrane

View Article Online
DOI: 10.1039/D6NR00934D

conductance potentiation as a function of the pulse number. Figure 5c concerns the PPF values as a function of Δt_0 parametrically in Δt. Note the maxima observed for intermediate values of Δt_0 suggesting that too short pulses cannot elicit significant electrical changes while large pulses give a saturation in the pore response.

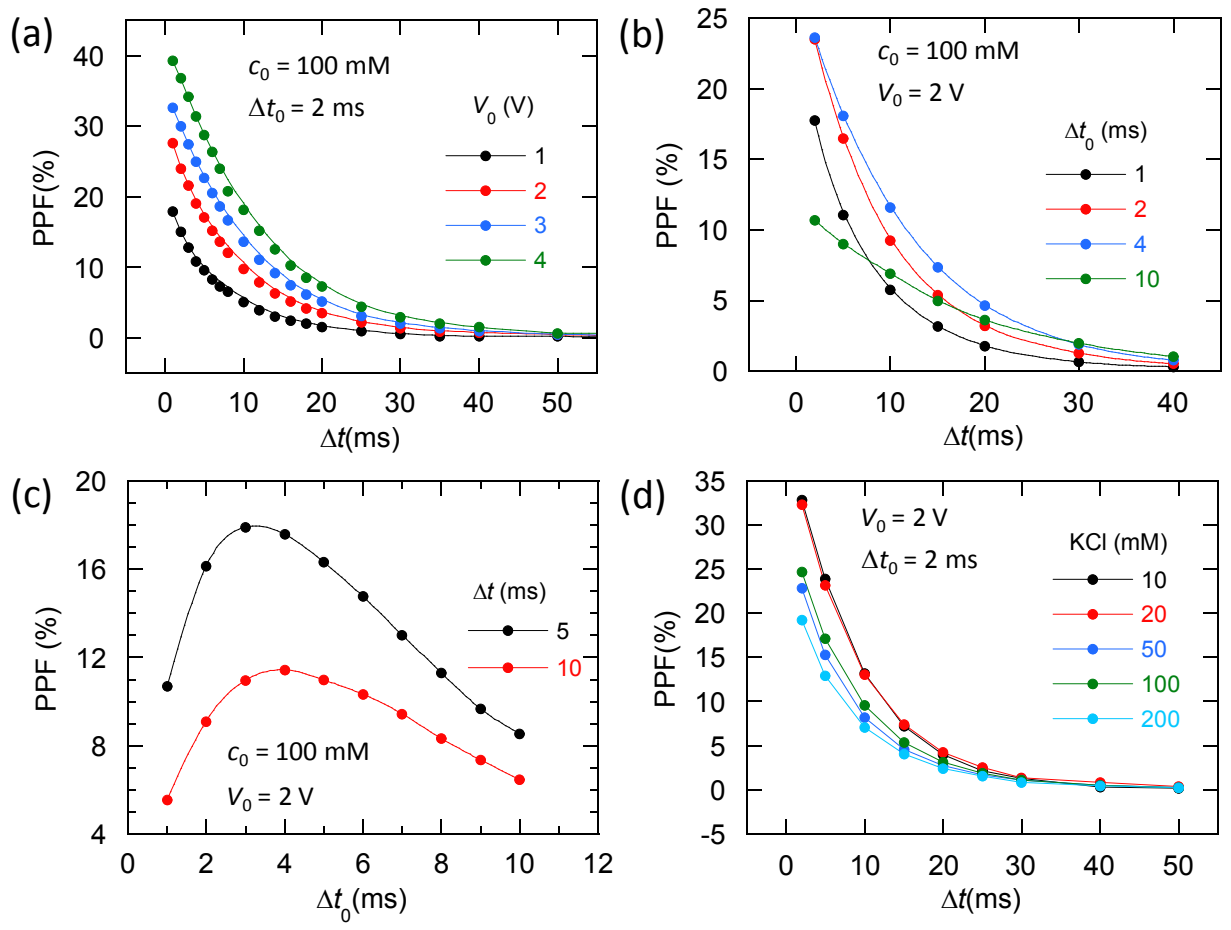

FIG. 5

(a) PPF – Δt curve for membrane sample #1 immersed in a c_0 = 100 mM KCl aqueous solution parametrically in the voltage amplitude V_0 with pulse time duration Δt_0 = 2 ms. (b) PPF – Δt curve parametrically in the pulse time duration Δt_0 for V_0 = 2 V and c_0 = 100 mM KCl. (c) PPF – Δt_0

View Article Online
DOI: 10.1039/D6NR00934D

curve parametrically in the time separation between pulses Δt for V_0 =2 V and c_0 = 100 mM KCl. (d) PPF– Δt curve parametrically in the KCl concentration c_0 for V_0 =2 V and Δt_0 = 2 ms.

We consider now two different applications of voltage pulses. In the first case, we demonstrate logical responses (Figures 6a and 6b) on the basis of the pulse parameters and pore response times of Figures 3–5 together with different solutions characteristics. In conical nanopores, the external solution *pH* values modulate the pore surface charges and the resulting ion accumulation and depletion phenomena that occurs at the pore tip.[2,26] This experimental procedure permits to modulate the *rectification polarity* simply by changing the *pore charge sign*. Thus, polarity-switchable ionic diodes can be obtained without mechanically reconfiguring the nanostructure, which provides a functional methodology at the circuit level (Figures 6a and 6b).

The combination of voltage *V* and *pH* as logical *inputs* can provide different logical *outputs* in terms of the distinct initial and final conductances that are observed at the beginning and end of the applied pulses. As an illustrative example,[20] Figure 6a shows a universal *NAND* logical function where the voltage *V* sign is the first *input*, the pH_{tip} is the second *input* (pH_{tip} = 7.0 for *input* 0 and pH_{tip} = 1.5 for *input* 1) and pH_{base} = 1.5 is kept constant. Here, *output* 0 corresponds to the absence of conductance potentiation and *output* 1 to the potentiation case. Figure 6b shows a *XOR* logical response obtained in the case of symmetrical solutions with $pH_{tip} = pH_{base}$ and ionic concentrations $c_{tip} = c_{base}$. In this case, it is the pore surface charge dependence on the *pH* that allows a chemical rather than an electrical gating.[20] Here, the *XOR* function can be implemented because the conductance potentiation is possible only for inputs (0, 1) and (1, 0).

View Article Online
DOI: 10.1039/D6NR00934D

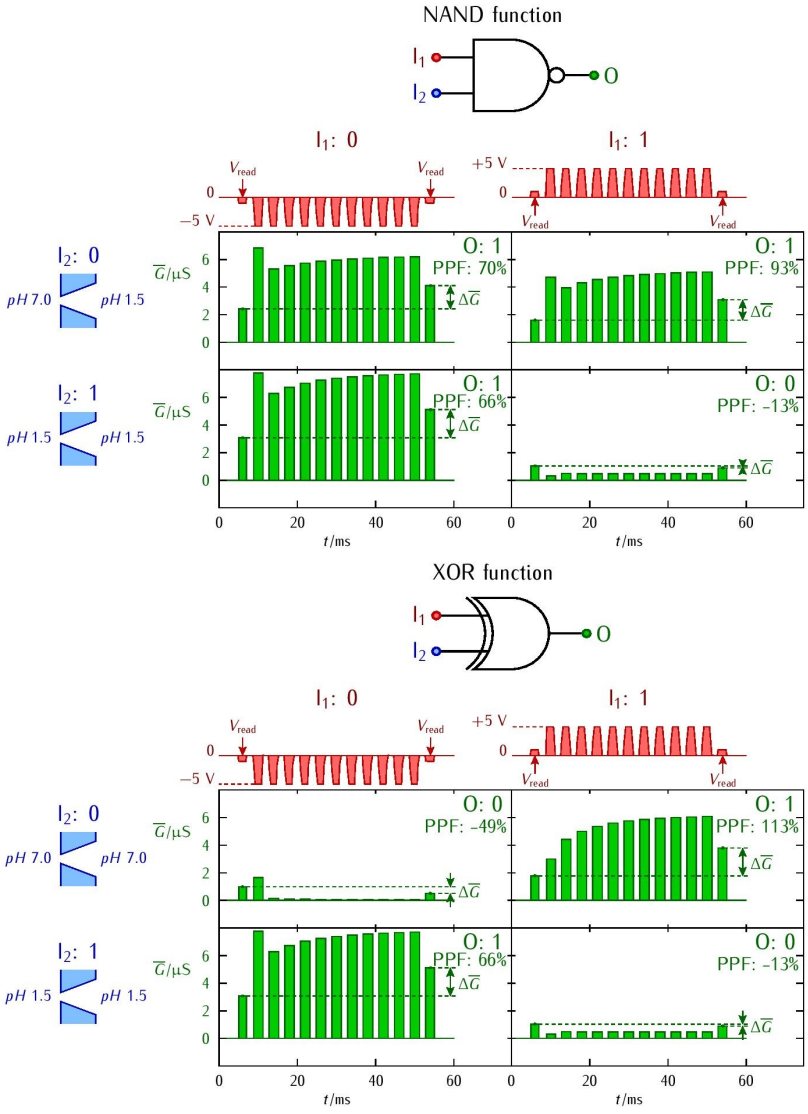

FIG. 6

(a) The voltage V sign and the solution pH_{tip}, *inputs* I_1 and I_2, give a *NAND* logic response in terms of the conductance, *output* O, in the case of a membrane (sample #3) of conical pores bathed in100 mM KCl solutions. The negative and positive voltage pulses result in the average conductance differences $\Delta\bar{G}$ for the different configurations. (b) The sign of V and the pH value of symmetrical

View Article Online
DOI: 10.1039/D6NR00934D

solutions (*inputs*) give a membrane conductance (*output*) that allows a *XOR* logic response. Data taken from Reference 20.

A second application combines *different voltage pulses* with *distinct individual membrane characteristics*. Here, we demonstrate a reservoir computing (RC) application of voltage pulse-learning phenomena by implementing a version of the tic-tac-toe game.[35] To this end, we simulate an artificial heterogeneous network consisting of individually different pore conductances that allows testing the array-level performance for more complex tasks in terms of the experimental behavior of single nanodevices.[14,16,35] This procedure permits to show the advantages of system variability and provides also useful information on the system scalability needed in practical applications.

We apply positive and negative voltage pulses to a parallel network of nanofluidic memristors, which are bathed in different ionic solution concentrations, acting as a heterogeneous reservoir (Figure 7). In this game, two players X and O compete to achieve a consecutive line on a 3 × 3 board. Because of the relatively low number of possible moves per player, it is feasible to train a RC network to learn the optimal move for every possible tic-tac-toe board using supervised-learning methods. Here, we use a parallel arrangement of N negatively charged conical nanopores at different ionic concentrations as the reservoir (Figure 7), which incorporates the system variability here. At this preliminary stage, the simulation constitutes a proof-of-concept based on an experimentally-motivated model. In particular, Figures 2 and 3 show that the theoretical results can reproduce the experimental potentiation phenomena observed in conical nanopores and their

View Article Online
DOI: 10.1039/D6NR00934D

electrochemical tuning. Note also that the full theoretical description of the memristive characteristics previously given in Reference 22 demonstrate further the validity of the basic concepts involved. Taking together, the above facts suggest that an experimental RC implementation should be feasible.

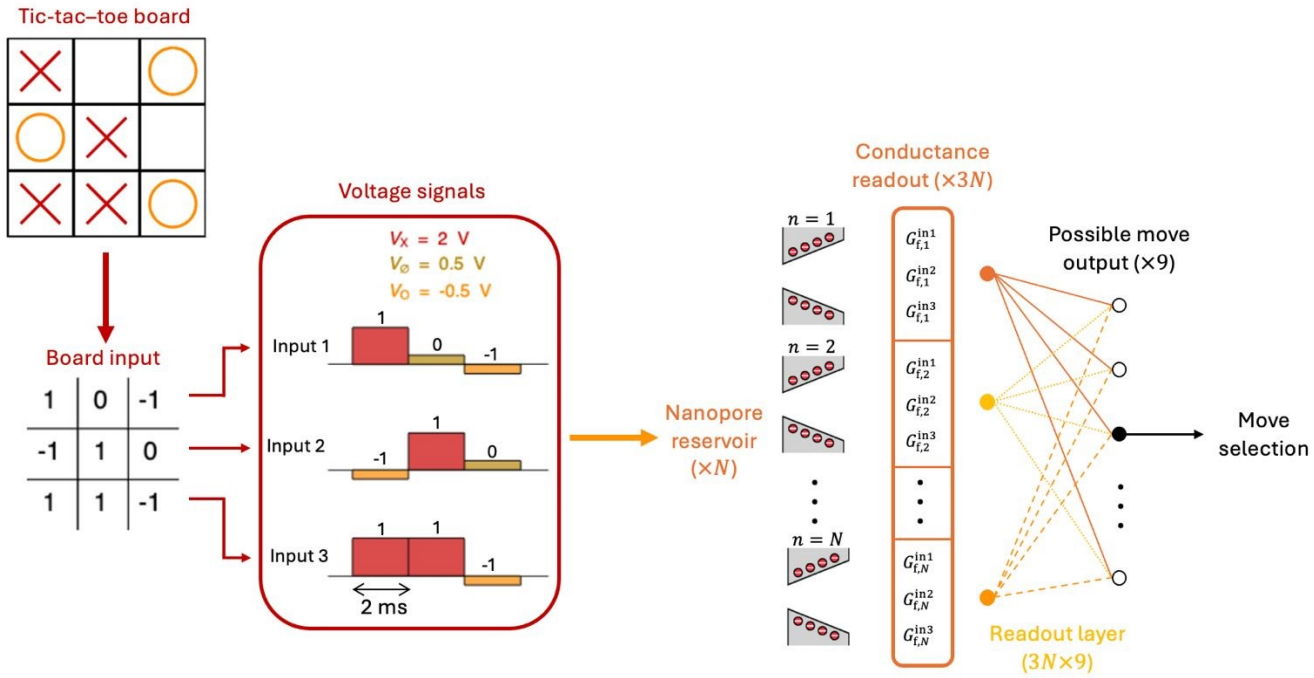

FIG. 7

RC scheme of the tic-tac-toe learning task. The 3 × 3 game boards are encoded in 3 × 3 sequences of 1, −1, and 0, depending on whether the corresponding box state is X, O, or is empty, respectively. The sequence is converted into three voltage signals, one for row, of three voltage pulses each. Thus, there are three input voltage signals for each board. Each signal represents a row on the board, and the signal pulses represent the respective boxes on the row. The input voltage of each pulse depends on the particular box state: $V_X = +2$ V, $V_O = -0.5$ V, and $V_\emptyset = +0.5$ V (empty

View Article Online
DOI: 10.1039/D6NR00934D

box, ∅). The three input signals for the corresponding board are applied to a parallel array of N nanopores bathed in KCl solutions of different concentrations $c_{0,i}$ (i = 1, ..., N) that are uniformly distributed between 10 and 120 mM. These individually different physico-chemical conditions account for the nanoscale variability of the array. The resulting $3N$ nanopore conductances at the end of the sequence for each row are taken as the readout signal. The final readout layer is trained using an embedding trees algorithm to select the corresponding optimal move from the nine possible moves. The game learning is conducted using supervised learning methods implemented here in a straightforward manner.

Note that, due to the short-time memory capabilities of the nanopores demonstrated in Figures 3–6, the final conductances for every row of Figure 7 are representative of each board (Figure 8). In our case, the significant rectification characteristics of the nanopores[26] allow encoding every possible board state using only three different voltages for the cell state that lead to distinct nanopore conductance states. In particular, a high positive voltage (V_X) gives a high pore conductance, a small positive voltage ($V_\emptyset$) permits to obtain the conductance without changing significantly the conductance state, and a negative voltage (V_O) results in a low conductance[26] From the final conductance characteristic of each board in Figure 7, a classification layer is trained to associate the readout signal of the board (Figure 8) with the corresponding optimal move. To test the training results, we perform a series of test games between the trained network and an ideal opponent. Here, a good training performance is indicated by the percentage of draws obtained by the network, since a draw is the best result that can be obtained when playing against an ideal opponent in the tic-tac-toe game.

View Article Online
DOI: 10.1039/D6NR00934D

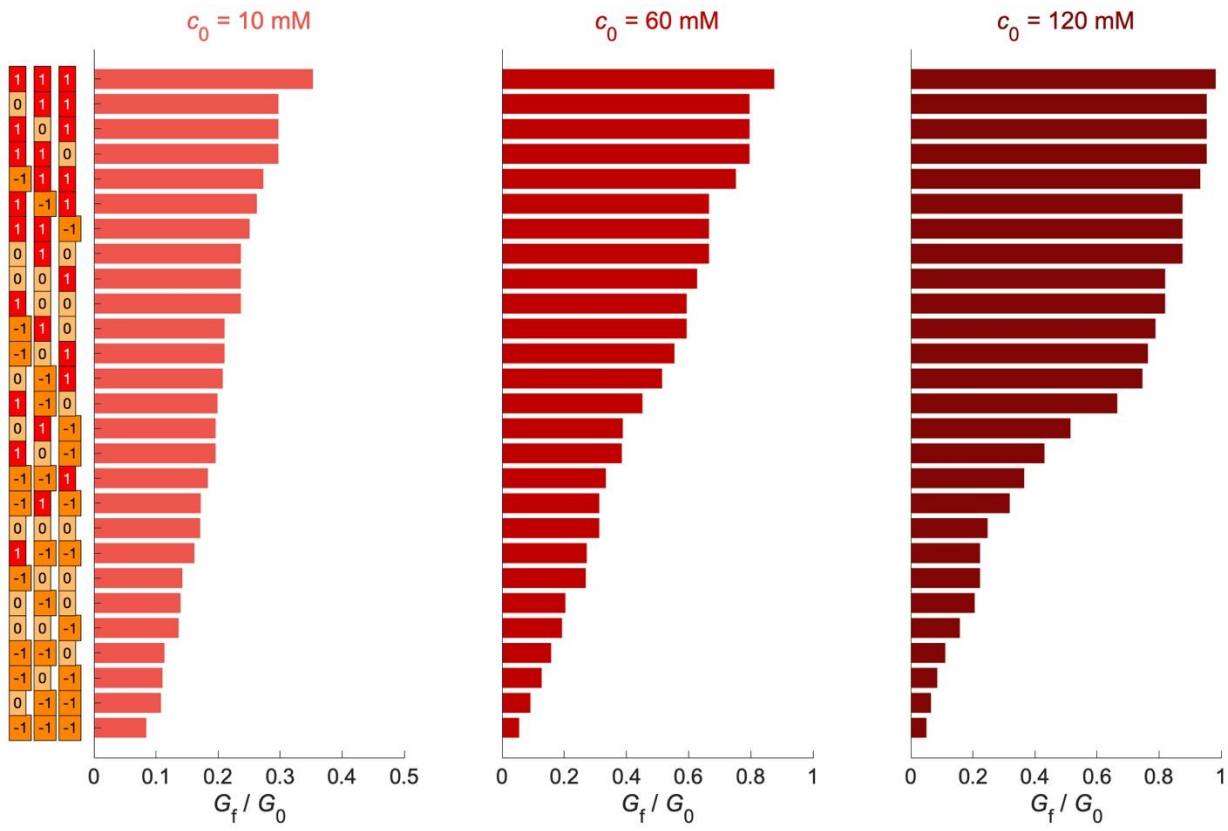

FIG. 8

Dimensionless final nanopore conductance values (G_f/G_0), where G_0 is a reference experimental conductance, computed for the $3^3 = 27$ possible rows of a tic-tac-toe board using three different ionic concentrations c_0 =10, 60, and 120 mM for the pores and the voltage protocol described in Figure 7. These different concentrations give the individually distinct pore conductances that simulate the array variability.

Figure 8 suggests that the different final memory states of the nanopores, characterized here by the final conductances achieved, provide an effective procedure to represent the distinct board rows. Indeed, while some final conductances G_f could be close to each other, this fact is not

View Article Online
DOI: 10.1039/D6NR00934D

a significant issue here because the readout representation of the board results from the combination of three rows and, in addition, individually different pore concentrations and conductances are used. Note that this high variability between the conductance representations of the different boards actually facilitates information processing and learning processes[14,49] (Figure 9).

To build the dataset, we select all tic-tac-toe boards that are not terminal, i.e., we consider only the boards where the game is still in progress. This selection is made because terminal boards are not suitable for game teaching using a supervised learning method. Also, we associate player O with the network, selecting only those boards where it is the turn of player O in the learning dataset. After these considerations, the total number of boards to be learnt is N_B = 2097. We associate with each board a label that represents the corresponding optimal move in this particular case. These labels are obtained from an ideal player that always chooses the optimal move using a brute force procedure. In this way, the learning dataset is formed by the $3N$-conductance readout of each board and the target move labels. A final readout layer is then trained using the embedding trees algorithm in order to associate each board conductance representation with the corresponding optimal move.

Figure 9 shows the training results of the classification layer obtained using the embedding trees algorithm in reservoirs with different N. As expected, increasing the number of nanopores in the array gives a better representation of the different boards, which eventually leads to high accuracies (Figure 9a). The results obtained with tests consisting of 1000 games played against an

View Article Online
DOI: 10.1039/D6NR00934D

ideal opponent clearly suggest the validity of the learning procedure, as shown by the draw percentages achieved by the trained network.

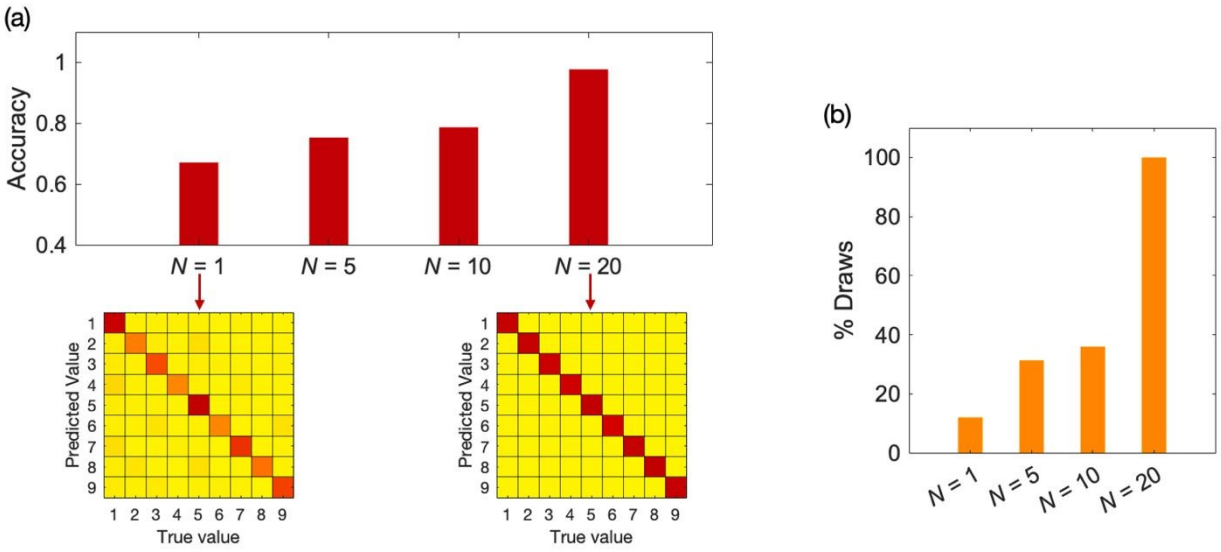

FIGURE 9

(a) Board learning accuracy for reservoirs with a different number N of nanopores. The resulting confusion matrices for $N = 1$ and $N = 20$. (b) The percentages of draws that are obtained by the trained network for tests of 1000 games played against an ideal opponent.

The results of Figures 8 and 9 suggest significant memory capabilities of nanofluidic conical pores. Using voltage pulses to encode the game information, the short-time memory of the nanopores permit to discriminate among the different boards, thus allowing the implementation of an RC scheme able to perform a multi-class classification and learn the most optimal move for every possible board configuration with good accuracies using a limited number ($N = 20$) of nanopores acting as reservoir nodes. Also, due to the rectifying properties of the asymmetrical

View Article Online
DOI: 10.1039/D6NR00934D

nanopores, the board information can be encoded using sequences of three different voltage states, which can provide an advantage with respect to the usual symmetrical responses where information encoding is limited to binary voltage sequences.

IV. CONCLUSIONS

Nanofluidic memristors exhibit conductance memory effects that provide useful options for neuromorphic computing, an emerging technology reminiscent of brain synapse plasticity that allows connection strength changes in response to electrical pulses. We describe here different procedures to modulate the nanofluidic conductance of conical pores by series of voltage pulses. Here, the spatio-temporal distribution of the mobile ions that modulates the pore conductance depends not only on the ionic concentration but also on the characteristics (amplitude, duration, and frequency) of the voltage pulses. The resulting history-dependent conductance allows short-term memory states and learning procedures through potentiation (connection strengthening due to ionic accumulation) and depression (connection weakening due to ionic depletion) effects that depend on the history of the voltage pulses. In this way, arrangements of nanofluidic memristors can be used in electrochemical circuits that allow logical responses and pattern learning from series of voltage pulses.

ACKNOWLEDGMENTS

J.C., J.A.M., S.M., and P.R. acknowledge the support from the *Ministerio de Ciencia e Innovación* (Spain) and the European Regional Development Funds (FEDER), project PID2022-

View Article Online
DOI: 10.1039/D6NR00934D

139953NB-I00. S.P. acknowledges the support from the *Conselleria d'Educació, Universitats i Ocupació* (*Generalitat Valenciana*). J.B. acknowledges the support from the European Research Council (ERC) via Advanced Grant No. 101097688 (PeroSpiker).

AUTHOR DECLARATIONS

Conflicts of Interest

The authors have no conflicts to disclose.

Author Contributions

S. Portillo: conceptualization, investigation, formal analysis, writing – original draft. **J. Cervera:** formal analysis, writing – review & editing, supervision, project administration, funding acquisition. **J. A. Manzanares:** formal analysis, writing – review & editing. **J. Bisquert**: formal analysis, writing – review & editing. **S. Mafe:** conceptualization, formal analysis, writing – original draft. **P. Ramírez:** conceptualization, investigation, formal analysis, supervision, writing – review & editing.

DATA AVAILABILITY

The data that support the findings of this study are available from the corresponding author under reasonable request.

View Article Online
DOI: 10.1039/D6NR00934D

REFERENCES

[1] E. Cao and Z. S. Siwy, "Leaving constraints of single nanopores and designing biomimetic nanopore arrays," Curr. Opin. Electrochem. **51**, 101677 (2025).

[2] P. Ramirez, V. Garcia-Morales, V. Gomez, M. Ali, S. Nasir, W. Ensinger, and S. Mafe, "Hybrid circuits with nanofluidic diodes and load capacitors," Phys. Rev. Appl. **7**, 064035 (2017).

[3] G. Pérez-Mitta, M. E. Toimil-Molares, C. Trautmann, W. A. Marmisollé, and O. Azzaroni, "Molecular Design of Solid-State Nanopores: Fundamental Concepts and Applications," Adv. Mater. **31**, 1901483 (2019).

[4] P. Ramirez, J. A. Manzanares, J. Cervera, V. Gomez, M. Ali, I. Pause, W. Ensinger, and S. Mafe, "Nanopore charge inversion and current-voltage curves in mixtures of asymmetric electrolytes," J. Membrane Sci. **563**, 633–642 (2018).

[5] G. Perez-Mitta, A. G. Albesa, C. Trautmann, M. E. Toimil-Molares,, and O. Azzaroni, "Bioinspired integrated nanosystems based on solid-state nanopores: "iontronic" transduction of biological, chemical and physical stimuli," Chem. Sci., 890–913 (2017).

[6] P. Robin, T. Emmerich, A. Ismail, A. Niguès, Y. You, G.-H. Nam, A. Keerthi, A. Siria, A. K. Geim, B. Radha, and L. Bocquet, "Long-term memory and synapse-like dynamics in two-dimensional nanofluidic channels," Science **379**, 161–167 (2023).

[7] T. M. Kamsma, J. Kim, K. Kim, W. Q. Boon, C. Spitoni, J. Park, and R. van Roij, "Brain-inspired computing with fluidic iontronic nanochannels," Proc. Natl. Acad. Sci. U.S.A. **121**, e2320242121 (2024).

[8] Q. Fan, J. Shang, X. Yuan, Z. Zhang, and J. Sha, "Emerging Liquid-Based Memristive Devices for Neuromorphic Computation," Small Methods, 2402218 (2025).

[9] C. S. Law, J. Wan, K. Nielsch, A. D. Abell, J. Bisquert, and A. Santos, "Recent advances in fluidic neuromorphic computing," Appl. Phys. Rev. **12**, 021309 (2025).

View Article Online
DOI: 10.1039/D6NR00934D

[10] K. Yang, J. J. Yang, R. Huang, and Y. Yang, "Nonlinearity in Memristors for Neuromorphic Dynamic Systems," Small Sci. **2**, 2100049 (2022).

[11] Z. Liu, H. Zhang, D. Liu, T. Sui, and Y. Qiu, "Modulation of Memristive Characteristics by Dynamic, Nanoprecipitation Inside Conical Nanopores," Small Methods, e01205 (2025).

[12] Y. Ling, L. Yu, Z. Guo, F. Bian, Y. Wang, X. Wang, Y. Hou, and X. Hou, "Single-Pore Nanofluidic Logic Memristor with Reconfigurable Synaptic Functions and Designable Combinations," J. Am. Chem. Soc. **146**, 14558–14565 (2024).

[13] G. Xu, M. Zhang, T. Mei, W. Liu, L. Wang, and K. Xiao, "Nanofluidic Ionic Memristors," ACS Nano **18**, 19423–19442 (2024).

[14] S. Portillo, P. Ramirez, S. Mafe, and J. Cervera, "Neuromorphic Reservoir Computing with Memristive Nanofluidic Diodes," Nano Lett. **25**, 9928–9934 (2025).

[15] G. Di Muccio, G. Paulo, L. Iannetti, A. Sauciuc, G. Maglia, and A. Giacomello, "Electrodrying in nanopores: from fundamentals to iontronic and memristive applications," arXiv:2512.14631v1.

[16] M. Jahangeer, J. Guo, Z. Qin, et al., "Memory Effects With Broken Symmetry in Nanofluidic Memristor for Neuromorphic Computing," Adv. Funct. Mater., e25932 (2025).

[17] K. Liu, Y. Wang, M. Sun, J. Lu, D. Shi, and Y. Xie, "Resistance-Restorable Nanofluidic Memristor and Neuromorphic Chip," Nano Lett. **25**, 6530–6538 (2025).

[18] Y. Niu, Y. Ma, and Y. Xie. "Soft Memristor at a Microbubble Interface," Nano Lett. **24**, 10475–10481 (2024).

[19] W. Wang, Y. Liang, Y. Ma, D. Shi, and Y. Xie, "Memristive Characteristics in an Asymmetrically Charged Nanochannel," J. Phys. Chem. Lett. **26**, 6852–6858 (2024).

[20] S. Portillo, J. Cervera, S. Mafe, and P. Ramirez, "Reversible logic with a nanofluidic memristor." Phys. Rev. E **110**, 065101 (2024).

View Article Online
DOI: 10.1039/D6NR00934D

[21] Z. Liu, L. Ma, H. Zhang, J. Zhuang, J. Man, Z.S. Siwy, and Y. Qiu, "Dynamic Response of Ionic Current in Conical Nanopores," ACS Appl. Mater. Interfaces **16**, 30496−30505 (2024).

[22] J. Cervera, S. Portillo, P. Ramirez, and S. Mafe, "Modeling of memory effects in nanofluidic diodes," Phys. Fluids **36**, 047129 (2024).

[23] W. Wang and Y. Ma, "An iterative approach to memristor," Phys. Fluids **37**, 082056 (2025).

[24] P. Y. Apel, Y. E. Korchev, Z. Siwy, R. Spohr, and M. Yoshida, "Diode-like single-ion track membrane prepared by electro-stopping," Nucl. Instrum. Methods Phys. Res., Sect. B **184**, 337–346 (2001).

[25] T. Ma, J. M. Janot, and S. Balme, "Track-etched nanopore/membrane: from fundamental to applications," Small Methods **4**, 2000366 (2020).

[26] J. Cervera, B. Schiedt, R. Neumann, S. Mafe, and P. Ramirez, "Ionic conduction, rectification, and selectivity in single conical nanopores." J. Chem. Phys. **124**, 104706 (2006).

[27] Y. Hou, Y. Ling, Y. Wang, M. Wang, Y. Chen, X. Li, and X. Hou, "Learning from the brain: Bioinspired nanofluidics," J. Phys. Chem. Lett. **14**, 2891–2900 (2023).

[28] T. M. Kamsma, E. A. Rossing, C. Spitoni, and R. van Roij, "Advanced iontronic spiking modes with multiscale diffusive dynamics in a fluidic circuit," Neuromorph. Comput. Eng. **4**, 024003 (2024).

[29] M. Ali 1, P. Ramirez, S. Nasir, J. Cervera, S. Mafe, and W. Ensinger, "Ionic circuitry with nanofluidic diodes," Soft Matter **15**, 9682–9689 (2019).

[30] M. Ali, P. Ramirez, I. Duznovic, S. Nasir, S. Mafe, and W. Ensinger, "Label-free histamine detection with nanofluidic diodes through metal ion displacement mechanism," Colloids Surf. B: Biointerfaces **150**, 201–208 (2017).

[31] J. S. Najem, G. J. Taylor, R. J. Weiss, M. S. Hasan, G. Rose, C. D. Schuman, A. Belianinov, C. P. Collier, and S. A. Sarles, "Memristive Ion Channel-Doped Biomembranes as Synaptic Mimics," ACS Nano **12**, 4702−4711 (2018).

View Article Online
DOI: 10.1039/D6NR00934D

[32] A. Noy, Z. Li, and S. B. Darling, "Fluid learning: Mimicking brain computing with neuromorphic nanofluidic devices," Nano Today **53**,102043 (2023).

[33] B. Sabbagh, N. Fraiman, A. Fish, and G. Yossifon, "Designing with iontronic logic gates-from a single polyelectrolyte diode to an integrated ionic circuit," ACS Appl. Mater. Interfaces, **15**, 23361–23370 (2023).

[34] N. E. Fraiman, B. Sabbagh, G. Yossifon, and A. Fish, "Toward an ion-based large-scale integrated circuit: design, simulation, and integration," Commun. Eng. **4**, 180 (2025).

[35] Z. Li, S. K. Myers, J. Xiao, Y. Li, N. Noy, A. Leuski, and A. Noy, "Neuromorphic ionic computing in droplet interface synapses," Sci. Adv. **11**, eadv6603 (2025).

[36] A. P. dos Santos, F. Jiménez-Ángeles, A. Ehlen, and M. Olvera de la Cruz, "Modulation of ionic conduction using polarizable surfaces," Phys. Rev. Research **5**, 043174 (2023).

[37] Q. Lu, F. Sun, L. Liu, L. Li, Y. Wang, M. Hao, Z. Wang, S. Wang, and T. Zhang, "Biological receptor-inspired flexible artificial synapse based on ionic dynamics," Microsyst. Nanoeng. **6**, 84 (2020).

[38] A. Ismail, G.-H. Nam, A. Lokhandwala, S. V. Pandey, K. V. Saurav, Y. You, H. Jyothilal, S. Goutham, R. Sajja, A. Keerthi, and B. Radha, "Programmable memristors with two-dimensional nanofluidic channels," Nat Comm. **16**, 7008 (2025).

[39] N. V. Kukushkin, R. E. Carney, T. Tabassum, and T. J. Carew, "The massed-spaced learning effect in nonneural human cells," Nat. Comm. **15**, 9635 (2024).

[40] P. Smolen, Y. Zhang, and J. H. Byrne, "The right time to learn: mechanisms and optimization of spaced learning," Nat. Rev. Neurosci. **17**, 77 – 88 (2016).

[41] N. Rouleau, D. M. Cairns, W. Rusk, M. Levin, and D. L. Kaplan, "Learning and synaptic plasticity in 3D bioengineered neural tissues," Neurosci. Lett. **750**, 135799 (2021).

View Article Online
DOI: 10.1039/D6NR00934D

[42] J. Cervera, A. Alcaraz, and S. Mafe, "Membrane Potential Bistability in Nonexcitable Cells as Described by Inward and Outward Voltage-Gated Ion Channels," J. Phys. Chem. B **118**, 12444–12450 (2014).

[43] J. Cervera, V. P. Pai, M. Levin, and S. Mafe, "From non-excitable single-cell to multicellular bioelectrical states supported by ion channels and gap junction proteins: Electrical potentials as distributed controllers," Prog. Biophys. Mol. Biol. **149**, 39e53 (2019).

[44] J. Cervera, M. Levin, and S. Mafe, "Multicellular adaptation to electrophysiological perturbations analyzed by deterministic and stochastic bioelectrical models," Sci. Rep. **14**, 27608 (2024).

[45] O. A. Polezhaeva, O. V. Kristavchuk, A. N. Nechaev, O. L. Orelovich, and P. Y. Apel, "Track-etched membranes as porous substrates with a preferential direction of capillary Flow," SSRN (2025). http://dx.doi.org/10.2139/ssrn.5849161

[46] P. Ramirez, J. Cervera, S. Nasir, M. Ali W. Ensinger, and S. Mafe, "Electrochemical impedance spectroscopy of membranes with nanofluidic conical pores," J. Colloid Interface Sci. **655**, 876–885 (2024).

[47] S. Mafé, V. Garcıa-Morales, and P. Ramírez, "Estimation of pKa shifts in weak polyacids using a simple molecular model: effects of strong polybases, hydrogen bonding and divalent counterion binding," Chem. Phys. **296**, 29–35(2004).

[48] G. Rivera-Sierra and J. Bisquert, "From pulses to plasticity: Analytical tools for memristive synapse design," APL Mach. Learn. **3**, 046102 (2025).

[49] J. Cervera, J. M. Claver, and S. Mafe, "Individual Variability and Average Reliability in Parallel Networks of Heterogeneous Biological and Artificial Nanostructures," IEEE Trans. Nanotech. **12**, 1198–1205 (2013).

View Article Online
DOI: 10.1039/D6NR00934D

Data availability statement

The data that support the findings of this study are available from the corresponding author under reasonable request.